Title

Optimal inverter sizing considering cloud enhancement

Permalink

https://escholarship.org/uc/item/0hf5w47t

Journal

Solar Energy, 86(1)

ISSN

0038-092X

Authors

Luoma, Jennifer
Kleissl, Jan
Murray, Keenan

Publication Date

2012

DOI

10.1016/j.solener.2011.10.012

Peer reviewed

Optimal Inverter Sizing Considering Cloud Enhancement

Jennifer Luoma, Jan Kleissl, Keenan Murray

Dept. of Mechanical and Aerospace Engineering, University of California, San Diego

1. INTRODUCTION

Inverter saturation or 'clipping' refers to the rejection of power output by the inverter when the PV power production is larger than the inverter AC rating (P_I). When inverter saturation occurs, power output is capped at P_I. To cap the output power, the inverter adjusts the voltage and current towards open circuit conditions. Inverters have a maximum AC rating in order to protect the integrity of the electrical components from increased temperatures. Proper sizing of PV arrays to inverters ensures that the maximum amount of renewable energy can be produced at the lowest cost and saturation events, which also increase wear on the inverter, are minimized. The PV DC rating is defined as the maximum power output of the array determined at standard test conditions (STC: 1000 W m^{-2}, 25°C panel temperature, and 1.5 spectrum air mass). An inverter sizing ratio (defined as $R = P_I /$ PV DC rating at STC) of 0.6 to 1, depending on location, is generally recommended (Macedo and Zilles, 2007). For southern Europe (defined as latitudes 35-45°), an R of 0.85-1.0 is recommended (Nofuentes and Almonacid, 1999). Inverter sizing ratio recommendations are typically close to the PV DC rating of the array ($R = 1$), because it is often close to the highest output of fixed-axis panels during clear skies. While the incident solar irradiance on the panel slightly exceeds 1000 W m^{-2} for parts of the year at mid and low latitude sites, the higher panel temperature under these conditions decreases PV solar conversion efficiency at the same time by about 15% which means that clear sky PV panel output is rarely significantly higher than their DC rating. Exceptions are PV panels at high elevation where smaller air mass and panel temperature can lead to significantly larger power outputs. Clear sky exceedence refers to clear sky periods in which the power output of the panels exceeds the inverter AC rating.

Unlike the inverter, the solar PV panel output is not capped at the rated capacity but increases near linearly with the irradiance received beyond 1000 W m^{-2}. Currently, inverter sizing approaches do not consider the phenomenon of cloud enhancement. Cloud enhancement refers to an unobscured solar disk for which the diffuse component of irradiance is significantly increased due to surrounding clouds and measured irradiance temporarily exceeds expected clear sky irradiance (and sometimes even the solar constant, defined as the incident solar irradiance at one astronomical unit). An increase in measured global horizontal irradiance (GHI, the sum of direct and diffuse irradiance incident on a horizontal surface) of more than 50% above the clear sky GHI has been well documented (Schade et al., 2007; Zehner et al., 2010). At our site clear periods were most likely, but frequent cloud enhancement occurred. Cloud enhancement events are important to consider for determining an inverter sizing ratio as they introduce the potential for the PV DC power output to significantly exceed the rated DC power, albeit on short timescales.

Hence, both cloud enhancement and clear sky exceedence contribute to energy losses due to inverter saturation. In addition to inverter saturation, inverter and panel efficiency, wiring,

maximum power point tracking, and attenuation of incoming light due to panel soiling and shading, contribute to PV system energy losses.

This study seeks to quantify the energy loss over a year as a result of inverter saturation for PV arrays and inverters installed in San Diego, California using 1-sec irradiance data. Most PV performance models consider hourly averaged irradiance input and neglect the distribution of irradiance on shorter timescales. Consequently, cloud enhancement cannot be resolved and the energy losses will be underestimated unless 1-sec irradiance data is considered. Previously, the effects of irradiance characteristics on energy losses and inverter efficiency have been studied up to 10-sec resolution (Burger and Ruther, 2006). We will examine how much of the energy losses can be resolved with input data from 1-sec to 1-hr resolution. On the other hand, if a large array is connected to a single inverter, only some of the panels in the array will experience cloud enhancement while the remaining (possibly cloudy) panels could act to balance the overall irradiance received such that the inverter is not saturated. While ideally a dense spatial network of irradiance sensors should be setup to quantify this process, the spatial averaging effect can also be represented by filtering the irradiance time series in the time domain. Section 2 describes the methods and filtering of the irradiance time series. The energy losses at different averaging timescales and the optimum sizing ratio are shown in Section 3. Section 4 includes a discussion and Section 5 includes conclusions.

2. METHODOLOGY

2.1. Power and irradiance data

From the PV array and inverter system on the north side of Engineering Building Unit 2 (EBU2) located at 32.881324° North 117.232952° West (WGS84) (Fig.2), plane-of-array (POA) global irradiance (the sum of direct and diffuse irradiance incident on the plane of the tilted array, GI, measured with a Licor Li200X silicon pyranometer), AC power, and DC power (both from the inverter, measured to ANSI C12.20 (0.2%) and IEC 687 (0.2%) Accuracy Classes) were sampled every minute and averaged over 15 minute time intervals from Feb 1, 2009 to November 30, 2010. The PV array consists of 182 Kyocera KD 205 GX-LP panels, with a tilt of 20° and an azimuth angle of 225° connected to five SMA Sunny Boy inverters (three 7 kW and two 5 kW inverters, Table 1). The 7kW inverter circuit consists of 3 parallel strings of 14 panels in series. The 5kW inverter circuit consists of 2 parallel strings of 14 panels in series. Results for inverters of identical model type were similar, and thus only data from one of each inverter model types are presented. GHI was measured by a collocated meteorological station with 1-sec resolution using a Licor Li200X pyranometer. The Li200X pyranometers are specified by the manufacturer to be accurate to within 3% and have a stability of better than 2% per year. A dust-rejecting coating of the sensor diffuser avoids the need for daily cleaning. Sensor cleaning is carried out monthly, but has had no measurable effect on calibrations or instrument performance. Missing power output and GHI data for January, May, September, and November 2009 were replaced by data on the same days from 2010. No data were available for the 5kW inverter in either October 2009 or October 2010, so October results are omitted. Days with missing GHI data (4) were excluded from the analysis.

A characterization of the frequency of cloud enhancement events was conducted over a calendar year; 3.5% of the GHI measurements were at least 10% greater than the predicted clear sky GHI and 0.6% were at least 30% greater than the predicted clear sky GHI (Figure 1). Similar frequencies of clear sky exceedance (4.1% of GHI measurements were at least 10% greater than the predicted clear sky GHI) were documented at a site in Lauder, New Zealand (Pfister et al., 2003).

Table 1
Details of the solar PV setup on EBU2 and inverter models SMA SB7000 (7 kW) and SMA SB5000 (5 kW). (SMA Solar Technology).

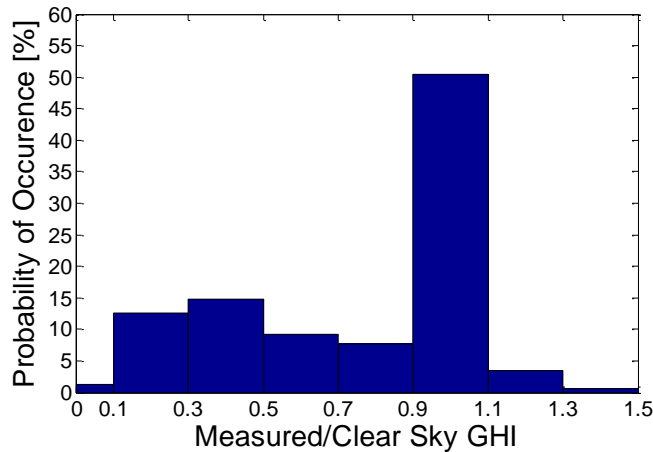| Inverter Model P_I	Number of Modules	Peak Inverter Efficiency	Manufacturer Recommended Rated PV DC Power	Installed Rated PV DC Power	Manufacturer Recommended R	Installed R
7 kW	42	97.1%	8750W	8610W	0.8	0.81
5 kW	28	96.8%	6250W	5740W	0.8	0.87

Figure 1: Probability of occurrence of the clear sky index for the EBU2 GHI site at San Diego, California (32.8813N, 117.2329W). The clear sky index was calculated by dividing 1 Hz GHI from a silicon pyranometer by the clear sky irradiance from the NREL Sunny Days Clear Sky Model (Gonzales and Wilcox, 2004; Long and Ackerman, 2000; implemented by Lave and Kleissl, 2011).

3

Figure 2: Aerial view of PV array and inverter system on the north side of Engineering Building Unit 2 (EBU2) located at 32.881324° North 117.232952° West (WGS84) (Map © 2011 Google – Map Data © 2011 Google)

2.2. Energy losses due to inverter saturation

The AC power output without saturation ($P_{AC,no\ sat}$) was calculated by multiplying a modeled total solar conversion efficiency η (sunlight to AC) by POA GI (where T is the frequency of the data) and the PV panel surface area A (Eq. 1)

$$P_{AC,no\ sat} = \eta GI_{POA}^{T}A. \tag{1}$$

A modeled η was computed as the average for the 45-min before the first saturation and 45-min after the last saturation on a given day. In this way, a constant η for the saturation period of each day (e.g. 1000-1700 PST on June 7 in Fig. 3) was applied to Eq. 1. Inverter saturation was assumed to occur when $P_{AC,no\ sat}$ was greater than the inverter AC power output rating (P_I).

Energy losses were defined as the difference between the actual inverter output (P_{AC}) and the modeled inverter output had the inverter not saturated and continued to perform at the same efficiency around when inverter saturation occurred ($P_{AC,no\ sat}$). Total energy losses due to saturation were calculated by integrating the energy loss for points in which $P_{AC,no\ sat}$ was greater than P_I (Fig. 3) as $\Sigma(P_{AC,no\ sat} - P_I)$ x 1-sec.
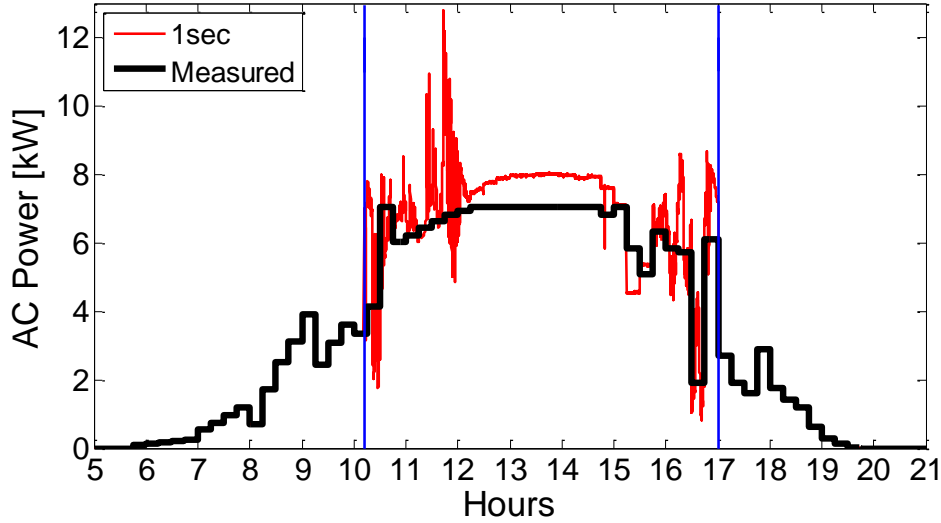
4

Figure 3: $P_{AC,no\ sat}$ (Eq. 1, 1-sec resolution) and measured P_{AC} for the 7 kW inverter for June 7, 2009 (15-min averages). Vertical blue lines indicate first and last occurrence of inverter saturation. Energy losses occur in clear skies from 1215-1515 PST and due to cloud enhancement from 1015-1215 and 1600-1700 PST.

2.3. Effects of time averaging on inverter saturation

High frequency (i.e. 1-sec) data are necessary to examine cloud enhancement effects as the duration of cloud enhancement events ranges from seconds to a few minutes (Pfister et al., 2003). In this section we describe how GI (and inverter losses) was calculated for different time scales. This allows (i) other investigators who have coarser data to quantify underestimation of energy losses and (ii) estimating the effect of spatial averaging of GI over a large PV array on reducing cloud enhancement effects and resulting energy losses.

Since GI (GI_{POA}^{15min}) and PV output P_{AC} were only available as measured 15-min averages, higher resolution data at averaging time T, GI_{POA}^{T}, were modeled using 1-sec GHI data. For example, to model 1-sec POA GI (GI_{POA}^{1sec}), the temporal variation of 1-sec GHI measurements (GHI^{1sec}) was added to a nearest-neighbor interpolated (piecewise-constant interpolant based on nearest value, Fig. 4a) 1-sec POA GI ($GI_{POA}^{15min \to 1sec}$). For shorter timescales (1 sec < T < 15 min), a running average of the 1-sec GHI measurements was calculated ($\langle GHI^{1sec} \rangle_T$, where <..> denotes time averaging). The deviation of this running average from a running average of GHI$_{1sec}$ evaluated on a 15-min timescale was added to the interpolated POA GI measurements (Eq. 2, Fig. 4e)

$$GI_{POA}^{T} = GI_{POA}^{15min \to 1sec} + (\langle GHI^{1sec} \rangle_T - \langle GHI^{1sec} \rangle_{15min}). \tag{2}$$
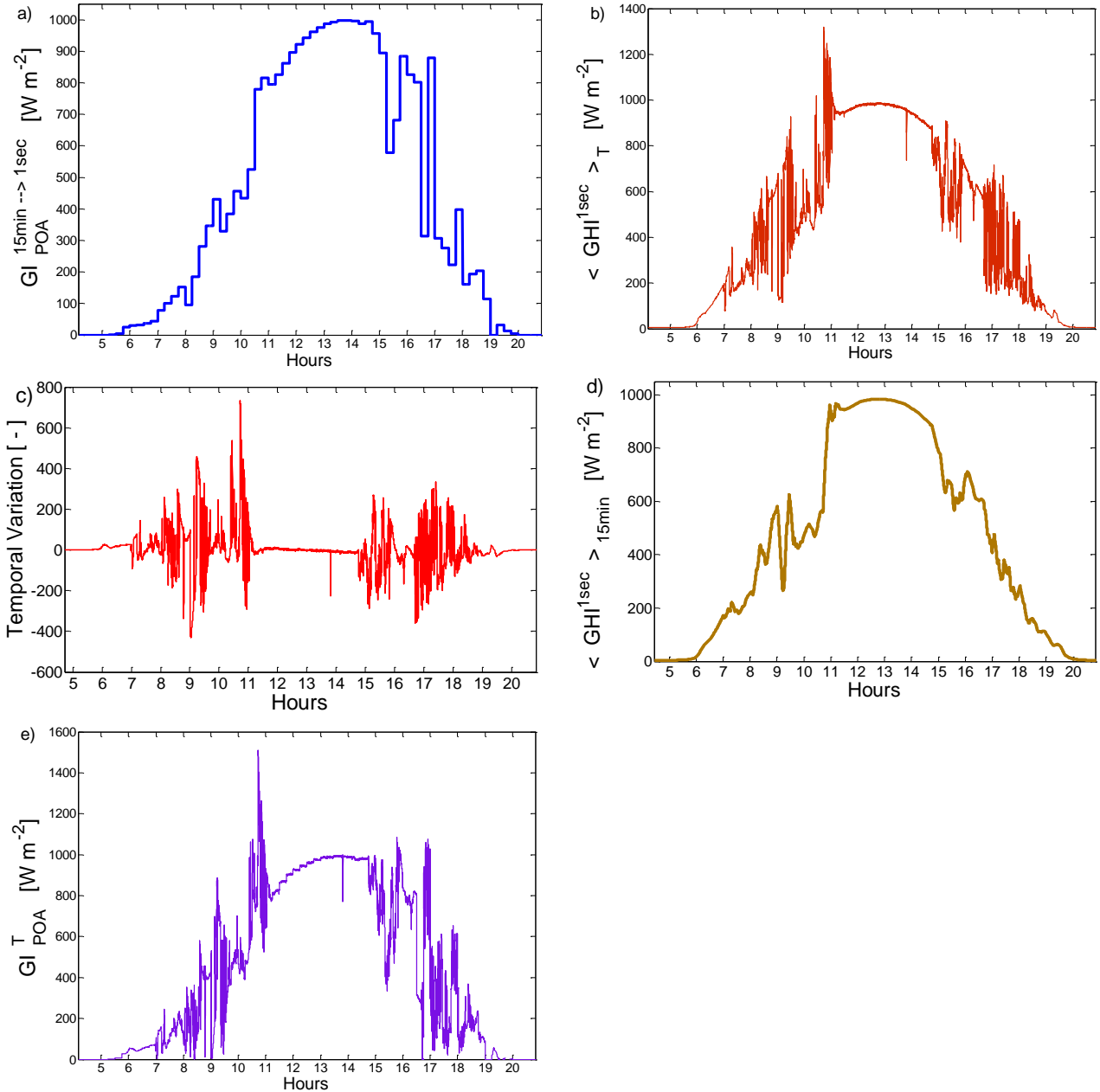
5

Figure 4: Process for constructing higher frequency GI_{POA}^{T} (e) for June 7th, 2009 for T = 1-sec. The measured 15-min GI is interpolated using nearest-neighbor ($GI_{POA}^{15min \rightarrow 1sec}$, a), a running average at 15-min of the 1-sec GHI ($\langle GHI^{1sec} \rangle_{T}$, b) is calculated ($\langle GHI^{1sec} \rangle_{15min}$, d), and the temporal variation (c) is found by taking the difference of (b) and (d); lastly, (c) is added to (a), resulting in the modeled GI_{POA}^{T} (e).

In doing this we assume equal variability of GHI and GI at 20° tilt. Since saturation usually occurs near solar noon and during cloud enhancement, direct irradiances for horizontal versus 20° tilted planes are usually within 10% (cos 20° = 0.94), and the diffuse irradiance is expected to depend on the location of the scattering cloud versus the sun and the sensor which is expected to be random. Total POA GI over a given day (June 7th, 2009) was 0.11% greater for the 1sec

6

modeled data as compared to the measured 15min data. Furthermore, we assume that PV output is linearly proportional to POA GI within the 15-min interval. Given near constant PV temperatures in a 15-min interval this is a reasonable assumption. Negative values of GI_{POA}^T, which occasionally occurred at the beginning and end of the day due to a large variation in GHI against a small POA GI, were set to zero; because this analysis focuses on energy losses due to inverter saturation (which occur around solar noon) this should not affect energy losses.

For an averaging time T of 15-min, GI_{POA}^{15min} was simply used for the energy loss analysis. Inverter saturation for input data averaged over $T > 15$-min can be calculated by averaging the GI and PV output directly

$$GI_{POA}^T = \langle GI_{POA}^{15min} \rangle_T. \tag{3}$$

Figure 5a depicts GI_{POA}^T for three averaging times on June 7, 2009. Between 1100-1200 PST, $GI_{POA}^{1\,sec}$ is up to 50% greater than 1000 W m^{-2} (the irradiance at which inverter DC ratings are determined). For the same time period, POA GI for 15-min and 1-h averaging times do not exceed 1000 W m^{-2}. Figure 5b shows the modeled AC power output for the 7 kW inverter at different T.
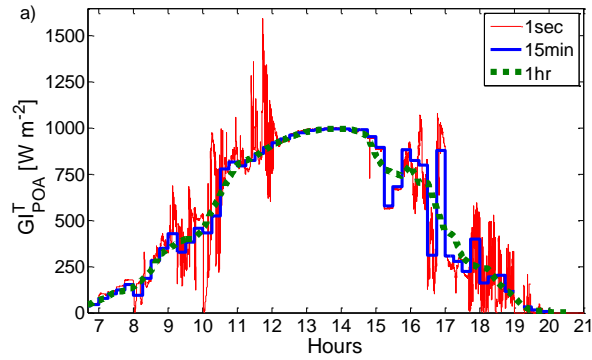

Figure 5a: POA GI for averaging times of 1-sec, 15-min, and 1-h for June 7, 2009.
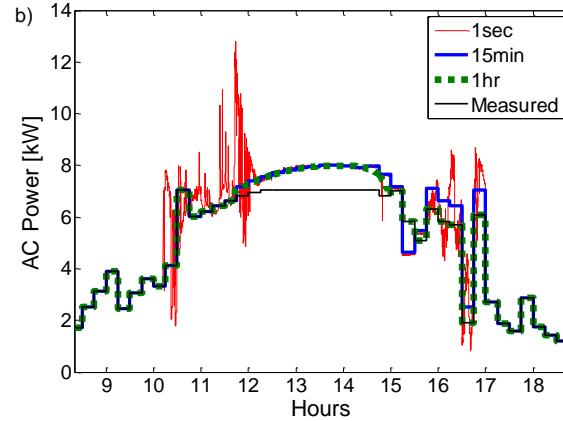
Figure 5b: Maximum AC power $P_{AC,no\,sat}$ and actual inverter AC power output for June 7, 2009.

2.4. Impacts of inverter size and inverter efficiency

Given the energy losses calculated using the modeled 1-sec GI POA data, an analysis of inverter size and inverter efficiency was conducted to determine optimal inverter sizing ratios. The largest $P_{AC,no\,sat}$ (Eq. 1) over the year would require $R=1.77$ for a 7 kW inverter. Inverter sizing ratios from 0.2 to 5.8 were simulated. The inverter conversion efficiency η_{AC} (DC to AC, Eq. 4) was modeled as a function of the power output over the inverter rating ($p_{out} = P_{AC}/P_I$, Fig. 6, Markvart and Castaner, 2006)

$$\eta_{AC} = \frac{p_{out}}{k_0 + (k_1+1)p_{out} + k_2 p_{out}^2}, \tag{4}$$

where k_0, k_1, k_2 are coefficients determined from a least squares fit. When operating at small p_{out}, an inverter is inefficient, η_{AC} peaks for $p_{out} = 0.5$, and decreases approximately 1% as p_{out} increases above 0.5 (Vignola et al., 2008). Thus, since η_{AC} is small at small p_{out}, dramatically increasing the size of the inverter to prevent all saturation losses may yield an overall decrease in energy production despite the fact that no inverter saturation occurs.
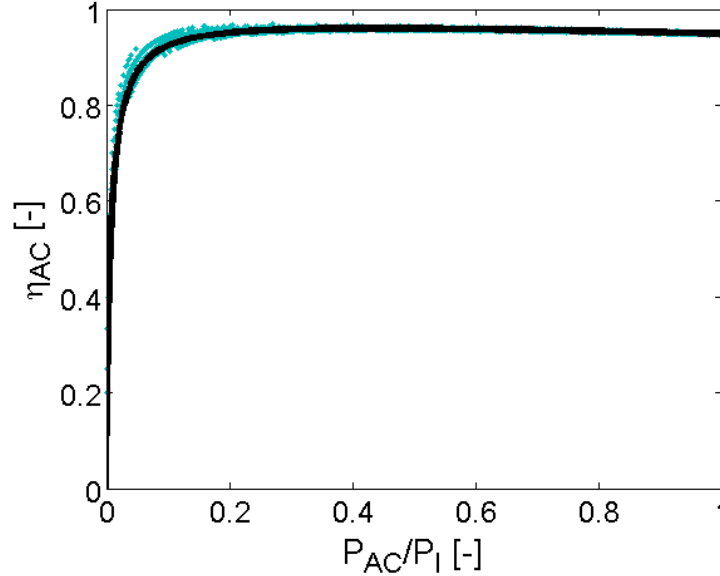

Figure 6: Inverter DC to AC conversion efficiencies η_{AC} versus the power output over the inverter rating at 15-min resolution over the year 2009 for the 7 kW inverter at EBU2 North. The black line is given by Eq. 4 with $k_0 = 0.007$, $k_1 = 0.009$, and $k_2 = 0.0375$.

The total solar irradiance to AC conversion efficiency η was separated into the inverter conversion efficiency η_{AC} (DC to AC, fit from Eq. 4) and PV panel efficiency (including line losses) η_{DC}, with $\eta = \eta_{DC}\eta_{AC}$. η_{DC} was assumed to be independent of inverter size and was calculated from the 15-min data using Eq. 5. During saturation events, to account for biased low η_{DC}, η_{DC} was averaged over the 45-min before the onset of saturation and 45-min after the end of saturation.

$$\eta_{DC} = \frac{\eta_{7kW}}{\eta_{AC}(P_{I7kW}, P_{AC,no\ sat})}. \qquad (5)$$

An inverter efficiency $\eta_{AC}(P_{AC,no\ sat})$ for each inverter size was calculated from Eq. 4 by inputting the new inverter size $(P_{I,model})$. The total solar conversion efficiency η for the PV array and inverter system was then calculated by multiplying the inverter efficiency by the panel efficiency determined by Eq. 6

$$\eta_{model} = \eta_{AC}(P_{I model}, P_{AC,no\ sat})\eta_{DC}. \qquad (6)$$

The new solar conversion efficiency η_{model} was multiplied by the POA GI and panel area to determine the theoretical AC power $(P_{AC,adj})$ for different inverter sizes (similar as in Eq. 1).

Figure 7 presents $P_{AC,no\ sat}$ and the modeled AC power considering η_{AC} of a 15.3 kW inverter ($P_{AC,adj}$). Both $P_{AC,adj}$ and $P_{AC,no\ sat}$ are similar in magnitude for June 7th, 2009 and indicate a daily energy output larger than the measured output. Close inspection reveals that the 15.3 kW inverter output is larger than the 7 kW inverter output near solar noon since it operates close to the optimum efficiency of the inverter (Fig. 6), but smaller in the morning. Our analysis allows quantifying the tradeoffs of different saturation losses and AC efficiencies for different inverter sizes over the year.
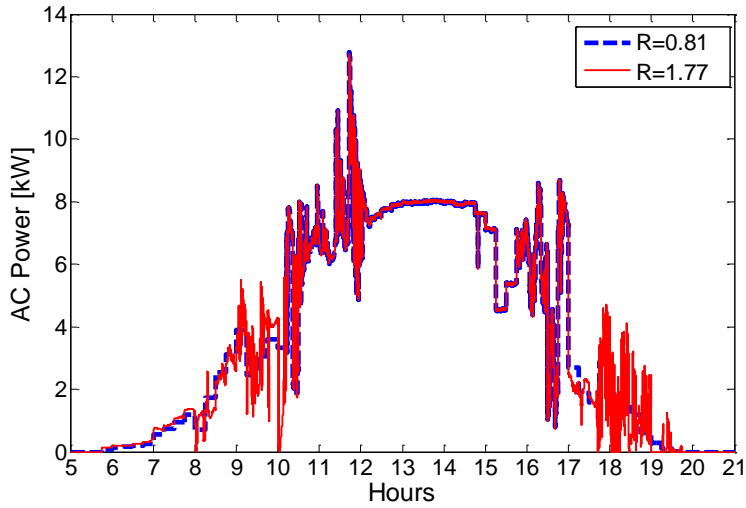

Figure 7: Modeled AC power $P_{AC,adj}$ for a simulated 15.3 kW inverter (*R*=1.77, Section 2.4) (for 1-sec data resolution), and $P_{AC,no\ sat}$ (*R*=0.81, Section 2.2) for June 7, 2009.

A limitation of this study is that we do not conduct power flow modeling of the PV array. During cloud-enhancement, large spatial variability of irradiance is expected and different panels on the same inverter may receive different amounts of irradiance. This will impact the maximum power point tracking of the inverter, as all panels are forced to operate at the same (globally optimal) voltage by the inverter. However, this voltage will decrease the conversion efficiency of individual panels and increase the energy loss.

3. RESULTS

Total monthly energy production, system efficiency, frequency of occurrence of cloud enhancement, and irradiation for the PV array and inverter system at EBU2 is shown in Fig. 8. Energy production was highest in May, July and August. This is a result of the 20° tilt and frequent marine layer cloudiness at the site in June. Energy losses (determined using 1-sec and 1-h POA GI in Eq. 1) were highest in the summer months (Fig. 9a) with a maximum in June and decreasing sharply for the other months. The overall losses are 6.5% in June and less than 4% in the other months. Energy losses that occur at 1-h averaging are representative of losses due to sustained inverter saturation presumably on those clear days when the solar beam is closest to perpendicular to the array (clear days in May through July, e.g. 1215-1515 PST in Fig. 5b). The difference between the energy losses over 1-h versus 1-sec can be attributed to cloud

9

enhancement. There is relatively poor correlation between energy losses and energy production (months with the highest energy production do not have the greatest energy losses, Fig. 8, Fig. 9). This suggests that energy losses are a result of complex processes.
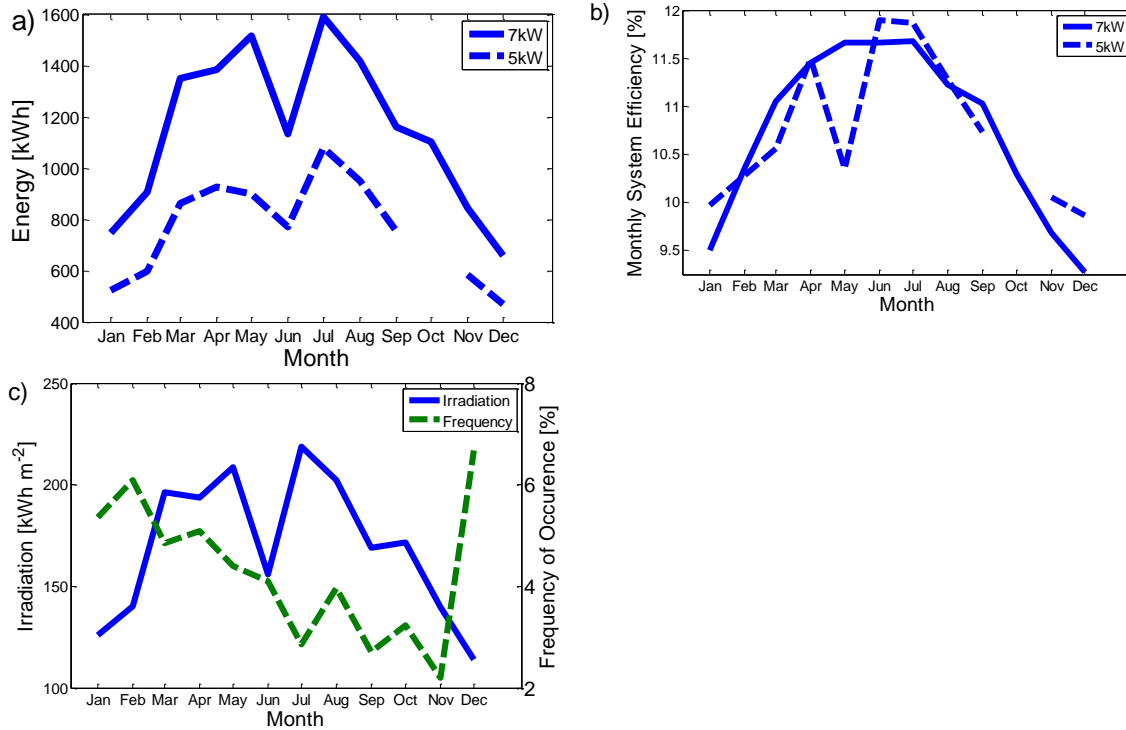

Figure 8: a) Total monthly AC energy production per inverter model, **b)** monthly system efficiency per inverter model, **c)** and monthly frequency of occurrence of cloud enhancement (greater than 10% of clear sky irradiance) and irradiation (GI) for an averaging time of 1-sec. Note outages for May (3 days) and October for the 5kW inverter.
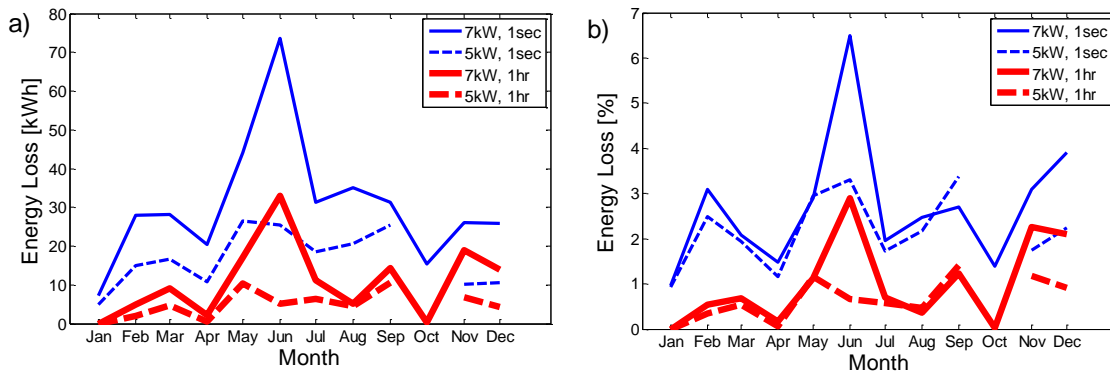

Figure 9: a) Energy loss and **b)** percent energy loss for each inverter model type for averaging times of 1-sec and 1-h.

The effects of averaging time T on energy losses can be seen in Fig. 10. From T of 1-sec to 1-h, the percentage of total yearly energy loss to total yearly energy production decreases from 2.65% and 2.20% for the 7 kW and 5 kW inverters, respectively, to less than 0.94% and 0.66%. This

10

indicates that smoothing of small timescale fluctuations in POA GI leads to underestimations of the energy losses due to inverter saturation. Yearly percent energy losses may be biased large due to missing AC power data in October (5 kW inverter only). Since energy losses are small in the winter months, inclusion of these time periods would presumably decrease the annual percent energy losses. As expected, Fig. 10 indicates that inverters with a smaller sizing ratio R experienced greater energy losses due to inverter saturation and that energy losses decrease with increasing averaging time. The magnitude of the slope decreases also with increasing averaging time.

As shown in Fig. 11, an optimal R can be determined by simulating η_{AC} for a series of inverter sizes. Considering 1-sec irradiance variations, $R = 1.22$ results in the largest energy production. The inverter efficiency decreases more rapidly for smaller inverter sizes (at $R = 0.72$, efficiency is more than 4% below optimal) than for larger sizes (at $R = 1.72$, efficiency is less than 0.4% below optimal). If hourly irradiance data is used, $R = 1.04$ results in the largest energy production (Fig. 12).
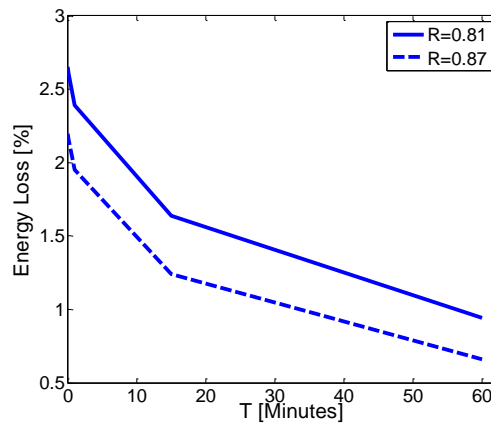

Figure 10: Percent annual energy loss and for each inverter type (Table 1). R in the legend is ratio of inverter maximum AC output rating divided by PV DC rating.
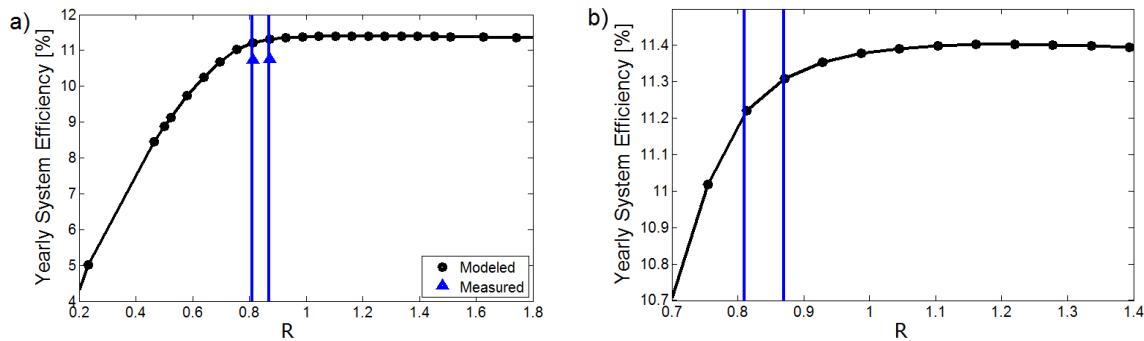

Figure 11: a) Yearly system efficiency $\eta = \eta_{DC}\,\eta_{AC}$ versus inverter sizing ratio R for 1-sec averaging time. A maximum yearly system efficiency occurs for R=1.22. Vertical lines show actual inverter sizing ratios (Table 1). Triangles indicate yearly system efficiencies using the measured 15-min averaged data for the two inverters (note yearly system efficiency for 5kW inverter excludes October). **b)** Zoom in to the region of largest η.
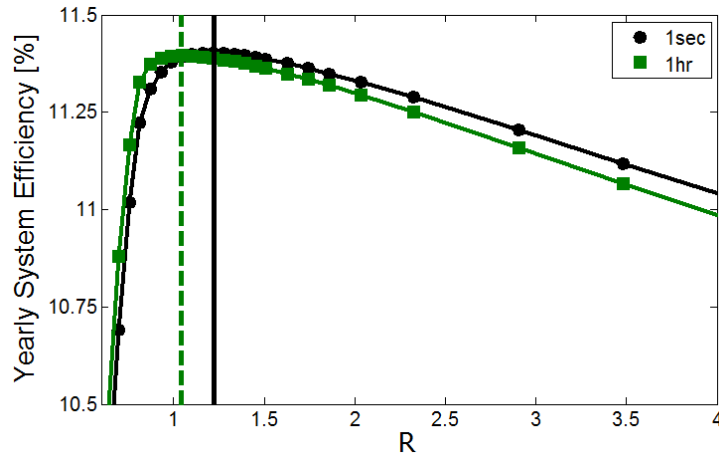
11

Figure 12: Yearly system efficiency versus R for 1sec and 1hr averaging time. Vertical lines show optimal R values for 1-sec ($R=1.22$, solid) and 1-hr ($R=1.04$, dashed) data.

4. DISCUSSION

This case study quantifies energy losses due to inverter saturation for a solar photovoltaic (PV) system. For a particular site with inverter sizing ratios of 0.81 and 0.87 in San Diego, California, up to 6.5% of the monthly energy production from a PV array and inverter system was lost due to inverter saturation (Fig. 9b). The losses were a combination of cloud enhancement effects and clear sky losses. On most cloud-free periods near solar noon in May through July, the 'smooth' power output curve already resulted in inverter saturation. While small in magnitude (less than 10% of the total energy production at any given time), these losses were persistent and occurred for up to 2 hours per day. On the other hand, cloud enhancement effects were short but caused losses up to 50% that occurred throughout the year and throughout the day.

An optimal inverter sizing ratio based on yearly system efficiency was determined to be 1.22 using 1-sec resolution data for our site and decreased to 1.04 using 1hr resolution data. Considering results from 1-sec data, changes in yearly system efficiency from the present sizing ratio to the optimal point were 1.6% (Fig. 11). For inverters larger than $R = 1.22$ saturation losses are reduced but the inverter operates more often in a low p_{out} regime reducing conversion efficiency (Fig. 6). For smaller inverters the conversion efficiency increases, but saturation losses increase until they reach 100% at an inverter size of zero. The effect on yearly system efficiency between a reasonable inverter sizing ratio ($0.8 < R < 3$) and the optimal inverter sizing ratio is less than 2% decrease compared to the optimum. The weak dependence of yearly system efficiency on inverter sizing ratio is consistent with previous studies (Nofuentes and Almonacid, 1999). In addition, the qualitative effect of irradiance measurement frequency on optimal inverter sizing ratio is consistent with results of Burger and Ruther ($R=0.83$ for 10-sec data and $R=0.74$ for 1hr data for a site in Freiburg, Germany). It is also illustrated that choosing a very large R can lead to significant decreases in yearly system efficiencies, so this a poor strategy both from an energy and economics perspective.

The 15-min averaged output data from the array filters out most cloud enhancement events since the peaks in the irradiance are counterbalanced by subsequent decreases due to cloud shading. This results in calculated losses of 38% less than for simulated 1-sec output data (for the 7kW inverter). Energy losses decreased by 65% (compared to the true losses at 1-sec for the 7kW inverter) when hourly GI was used (Fig. 10). This indicates that using hourly averaged data for inverter sizing can dramatically underestimate the energy losses due to saturation. These results strongly depend on R and location, in particular the frequency of cloud enhancement events during large irradiance periods. In regions like south-eastern California where the summers are predominantly cloud-free, the energy losses due to cloud enhancement are probably negligible. However, in regions with summer convective activity such as Florida, Texas, and parts of Arizona (Lave and Kleissl, 2010), the losses may be larger than in San Diego. Results also indicate that using hourly data impacts the optimum R value (Fig. 12). This shows that cloud enhancement events are important to consider when determining optimum inverter sizing ratios.

On the other hand, the spatial extent of large PV arrays also serves to reduce the number and intensity of saturation events due to cloud enhancement. Increasing averaging period by averaging small scale fluctuations of irradiance can be considered analogous to decreasing small scale fluctuations of irradiance by larger PV arrays. Thus, it can be expected that as the size of a PV array increases, the potential for cloud enhancement to cause large saturation energy losses decreases. Since cloud enhancement is a highly localized increase in irradiance (and is surrounded by decreased irradiance due to cloud shadows), the average irradiance over all PV panels connected to an inverter is substantially less than the extreme values measured with a small pyranometer. A simple filter that converts the 1-sec GHI timeseries at a point to the average irradiance over an array can be defined as

$$f = A^{1/2} / U \tag{7}$$

where U is the cloud velocity. The 7 kW arrays have 42 modules with a surface area of 60 m^2. Assuming a typical cloud advection velocity of 5 m s^{-1} (Chow et al., 2011), the filter size would be 1.5-sec. Consequently, for small arrays the energy losses calculated using the 1-sec data would be accurate. However, for a 300 kW array (and $U = 5$ m s^{-1}), the 10-sec averaged results are expected to be more representative.

This analysis simply focuses on quantifying the amount of energy loss and illustrating that energy could be gained by increasing the size of the inverter such that inverter saturation does not occur. Economic considerations are likely to indicate an optimal inverter sizing ratio less than $R = 1.22$. In addition, the effect of PV panel degradation (on the order of 0.5% loss of DC power rating per year for crystalline silicon panels) on the inverter sizing ratio needs to be considered. For our site, power data from the first year of installation was used, and the optimal inverter sizing ratio would likely be less than R=1.22 if the entire lifetime of the PV system was considered as inverter saturation would be less likely to occur as the effective PV DC rating decreases over time.

5. CONCLUSION

The importance of cloud enhancement extends beyond energy losses to issues such as inverter tripping and blown fuses at large solar PV plants. Consideration of cloud enhancement in determining an optimal inverter sizing ratio suggests that generally recommended values (*0.6<R<1*) yield energy losses as great as 2.65% of the total yearly energy production. Results show that increasing the inverter sizing ratio to *R=1.22* for the studied system would lead to the greatest yearly energy output. In addition, the wear on the inverter would be diminished as compared to the current installed system as the inverter would not undergo sustained stress from operating at a high percentage of its maximum power output. A holistic studied should be conducted including the capital cost and lifetime of the inverter in addition to system efficiency in order to determine the optimum *R* value.

References
Burger, B, Ruther, R, 2006. Inverter sizing of grid-connected photovoltaic systems in the light of local solar resource distribution characteristics and temperature. *Solar Energy*. 80, 32-45.

Chow CW, Urquhart B, Lave M, Kleissl J, 2011. Intra-hour forecasting with a Total Sky Imager at the UC San Diego Solar Energy Testbed. *Submitted to Solar Energy.*

Gonzales, C Wilcox S, 2004. Sunny Days. National Renewable Energy Laboratory.

Lave, M, Kleissl J, Arias-Castro E, 2011. High-frequency irradiance fluctuations and geographic smoothing. *Accepted pending minor revisions in Solar Energy*.

Lave, M, Kleissl J, 2010. Optimum fixed orientations and benefits of tracking for capturing solar radiation in the continental United States, *Renewable Energy*, 36(3), 1145-1152.

Long. CN, Ackerman, TP, 2000. Identification of clear skies from broadband pyranometer measurements and calculation of downwelling shortwave cloud effects. *J. Geophys*. Res. 105, 15609-15626.

Macedo, WN, Zilles, R, 2007. Operational Results of Grid-Connected Photovoltaic System With Different Inverter's Sizing Factors (ISF). *Prog. Photovolt: Res. Appl.* 15, 337-352.

Markvart, T, Castaner L, 2006. "IIIa-3: Review of System Design and Sizing Tools." *Practical Handbook of Photovoltaics Fundamentals and Applications*. Oxford: Elsevier, 544-61.

Pfister, G, McKenzie, R.L, Liley, JB, Thomas, A, Forgan, BW, Long, CN, 2003. Cloud Coverage Based on All-Sky Imaging and Its Impact on Surface Solar Irradiance. *J. Appl. Meteor.*, 42, 1421–1434.

Schade, NH; Macke, A, Sandmann, H, Stick, C, 2006. Enhanced Solar Global Irradiance During Cloudy Sky Conditions. *Meteorologische Zeitschrift*, 16.3, 295-303.

SMA Solar Technology. Data Sheet: SUNNYBOY5678-DUS100723 < http://www.sma-america.com/en_US/products/grid-tied-inverters/sunny-boy/sunny-boy-5000-us-6000-us-7000-us-8000-us.html>, accessed October 15, 2010.

Vignola, F, Mavromatakis, F, Krumsick, J, 2008. Performance of PV Inverters *Proc. of the 37th ASES Annual Conference,* San Diego, CA.

Zehner, M, Weigl, T, Weizenbeck, J, Mayer, B,Wirth, G, Prochaska, H, Giesler, B, Gottschalg, R, Becker, G, Mayer, O, 2010. Systematische Untersuchung meteorologischer Einstrahlungsereignisse, *25th PV Symposium*, Staffelstein, Germany.